

BNL--44534

DE90 011515

**BEAM-LINE CONSIDERATIONS FOR EXPERIMENTS WITH
HIGHLY-CHARGED IONS**

Brant M. Johnson

Atomic and Applied Physics Group

Department of Applied Science, Brookhaven National Laboratory

Upton, New York 11973

Invited Talk Presented at

Workshop on Atomic Physics at the Advanced Photon Source

Argonne National Laboratory, Argonne, Illinois

March 29-30, 1990

DISCLAIMER

This report was prepared as an account of work sponsored by an agency of the United States Government. Neither the United States Government nor any agency thereof, nor any of their employees, makes any warranty, express or implied, or assumes any legal liability or responsibility for the accuracy, completeness, or usefulness of any information, apparatus, product, or process disclosed, or represents that its use would not infringe privately owned rights. Reference herein to any specific commercial product, process, or service by trade name, trademark, manufacturer, or otherwise does not necessarily constitute or imply its endorsement, recommendation, or favoring by the United States Government or any agency thereof. The views and opinions of authors expressed herein do not necessarily state or reflect those of the United States Government or any agency thereof.

MASTER

FOR INFORMATION ON THIS DOCUMENT CONTACT

By acceptance of this article, the publisher and/or recipient acknowledges the US Government's right to retain a nonexclusive, royalty-free license in and to any copyright covering this paper.

Beam-Line Considerations for Experiments with Highly-Charged Ions*

Brant M. Johnson[†]
Department of Applied Science
Brookhaven National Laboratory, Upton, NY 11973

The APS offers exciting possibilities for a bright future in x-ray research. For example, measurements on the inner-shell photoionization of ions will be feasible using stored ions in ion traps or ion beams from an electron-cyclotron-resonance ion source, or perhaps even a heavy-ion storage ring. Such experiments with ionic targets are the focus for the discussion given here on the optimization of photon flux on a generic beamline at the APS. The performance of beam lines X26C, X26A, and X17 on the x-ray ring of the National Synchrotron Light Source will be discussed as specific examples of beam-line design considerations.

[†]with K.W. Jones, M. Meron, M.L. Rivers and P. Spanne (Department of Applied Science, Brookhaven National Laboratory) W.C. Thomlinson, D. Chapman and J. Hastings (National Synchrotron Light Source Department, Brookhaven National Laboratory).

*Research supported by the Chemical Sciences Division, Office of Basic Energy Sciences, US Department of Energy, under Contract No. DE-AC02-76CH00016.

In September of 1980 the "Workshop on Atomic Physics at the NSLS" was held at Brookhaven National Laboratory. Considerable interest and excitement was expressed for the potential impact on atomic, molecular and optical (AMO) physics research promised by the new National Synchrotron Light Source (NSLS), which was then under construction. Many of the conclusions and areas of interest evidenced in the proceedings of that workshop are still true today. For example, (1) the AMO physics community is much more interested in soft-x and VUV photons, than in hard x rays; (2) there have been very few measurements on the photoionization of ions, particularly for inner-shells; and (3) the next generation facility will undoubtedly enhance experimental capabilities in current research programs and foster the development of new research endeavors.

Experimental progress in the decade since the NSLS workshop is well documented in other contributions to this APS workshop. Some of the specific experiments performed on beam lines X26C at the NSLS are discussed or mentioned in the contributions by Dave Church, Bernd Crasemann, and Jon Levin. Some of this work was performed in collaboration with researchers from Texas A&M, the University of Tennessee and Oak Ridge National Laboratory, Argonne National Laboratory, and St. Etienne, FRANCE. Additional studies of synchrotron-radiation (SR) induced fluorescence spectroscopy and the direct inner-shell photoionization of ions from a conventional ion source are carried out by the local BNL group, but they will not be discussed here.

The relatively small number of practitioners in AMO physics with hard x rays is both a blessing and a curse. The good news is that the field is wide open with more exciting ideas and possibilities than current researchers can possibly investigate. The down side is just that - it has proved difficult to interest other experimenters (and funding agencies) to turn their attention toward hard x-ray research in AMO physics. Perhaps this workshop will serve as a catalyst to stimulate interest in the illuminating possibilities that the APS, the ESRF, and the SPring-8 will offer.

Unquestionably, the new third generation hard x-ray photon sources will provide substantially more x rays than second generation machines (such as the NSLS x-ray ring). However, experimental beam lines must be carefully designed to realize the full potential of a third generation photon source. Figs. 1-2 give an overview of generic beam line considerations.

The specific characteristics of beam lines X26C and X26A, with particular emphasis on the performance of a 1:1 cylindrical focussing mirror, are discussed in Figs. 3-9. The relative performance of APS undulator A and bending magnet beamlines at the NSLS and APS are compared in Fig. 10 and discussed in Fig. 11 through the example of measurements of the radiation produced by the NSLS superconducting wiggler on port X17.

The PHOBIS concept for producing highly-charged ions through successive photoionization of trapped ions is reviewed in Figs. 12-13. Finally, an overview of a proposed heavy-ion storage ring for use at a hard x-ray light source is given in Figs. 14-24.

BIBLIOGRAPHY

ATOMIC PHYSICS RESEARCH ON BEAMLINE X26C AT THE NSLS

B. M. Johnson, M. Meron, A. Agagu, and K. W. Jones,
Nucl. Instrum. and Meth. B24/25 (1987) 391.

PROPOSAL FOR A HEAVY-ION STORAGE RING AT THE NSLS

K. W. Jones, B. M. Johnson, M. Meron, Y. Y. Lee,
P. Thieberger, and W. C. Thomlinson,
Nucl. Instrum. and Meth. B24/25, (1987) 381.

K. W. Jones, B. M. Johnson, M. Meron, B. Crasemann,
Y. Hahn, V. O. Kostroun, S. T. Manson, and S. M. Younger,
Comments At. Mol. Phys. 20 (1987) 1.

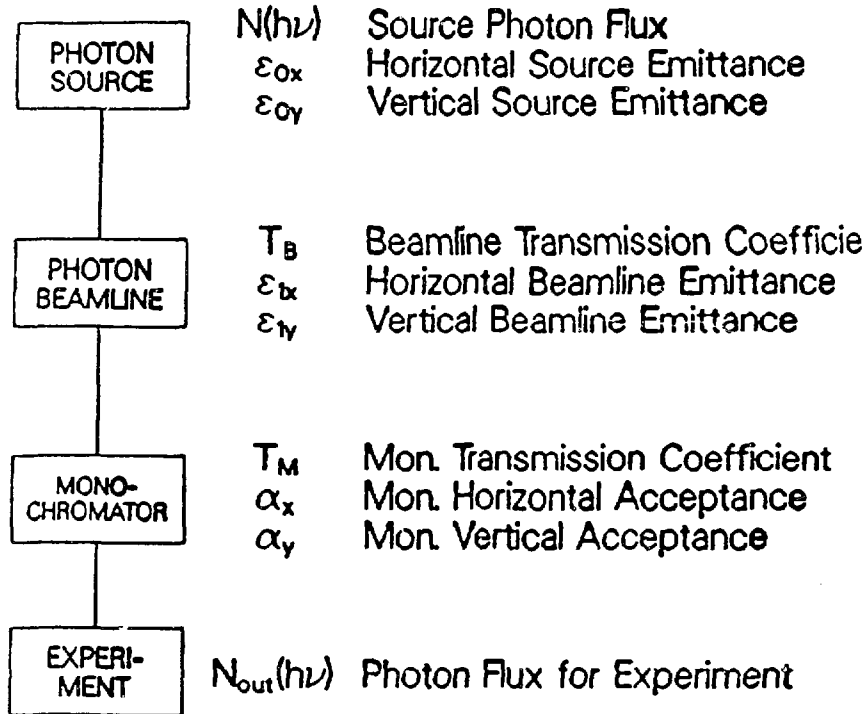
Feasibility Study (1988); DOE Conceptual Design Report (1989).

BASIC REFERENCES ON RESEARCH WITH SYNCHROTRON RADIATION

Introduction to Synchrotron Radiation by Giorgio Margaritondo,
Oxford University Press, New York (1988).

Handbook on Synchrotron Radiation, Ed. Ernst-Eckhard Koch,
North Holland Publishing Company, Amsterdam (1983).

GENERAL CONFIGURATION FOR SR EXPERIMENTS
after R.L. Johnson (pp. 173-260) in
Handbook on Synchrotron Radiation, Vol. 1A



$$N_{out}(\lambda) = N(\lambda) \theta_x T_B T_M (\alpha_x/\epsilon_{bx})(\alpha_y/\epsilon_{by})$$

Fig. 1 illustrates the relevant parameters that determine the photon flux $N_{out}(\lambda)$ available for an experiment. In the equation given at the bottom of the figure; θ_x is the horizontal divergence angle of emitted radiation from the bending magnet or insertion device of interest.

$$N_{\text{out}}(\lambda) = N(\lambda) \theta_x T_B T_M (\alpha_x/\epsilon_{1x})(\alpha_y/\epsilon_{1y})$$

TO MAXIMIZE PHOTON FLUX FOR A
SYNCHROTRON RADIATION EXPERIMENT:

1. Design Light Source for
MAXIMUM PHOTON FLUX
and MINIMUM EMITTANCES
(Horizontal and Vertical).
2. Design both beamline and
monochromator to accept
LARGEST POSSIBLE SOLID ANGLES.
3. MATCH ACCEPTANCES of mono-
chromator and beamline to
the emittance of the source.
4. MAXIMIZE TRANSMISSION of
beamline and monochromator.

Fig. 2 describes the design criteria for optimum photon flux on a generic synchrotron radiation (SR) beam line. As the equation from Fig. 1 implies, the source photon flux, θ_x , transmission of beam line and monochromator, and monochromator acceptance solid angles should be maximized, while the emittance of the source and beam line are minimized. A fuller description of this and other considerations are given in the general references listed in the bibliography.

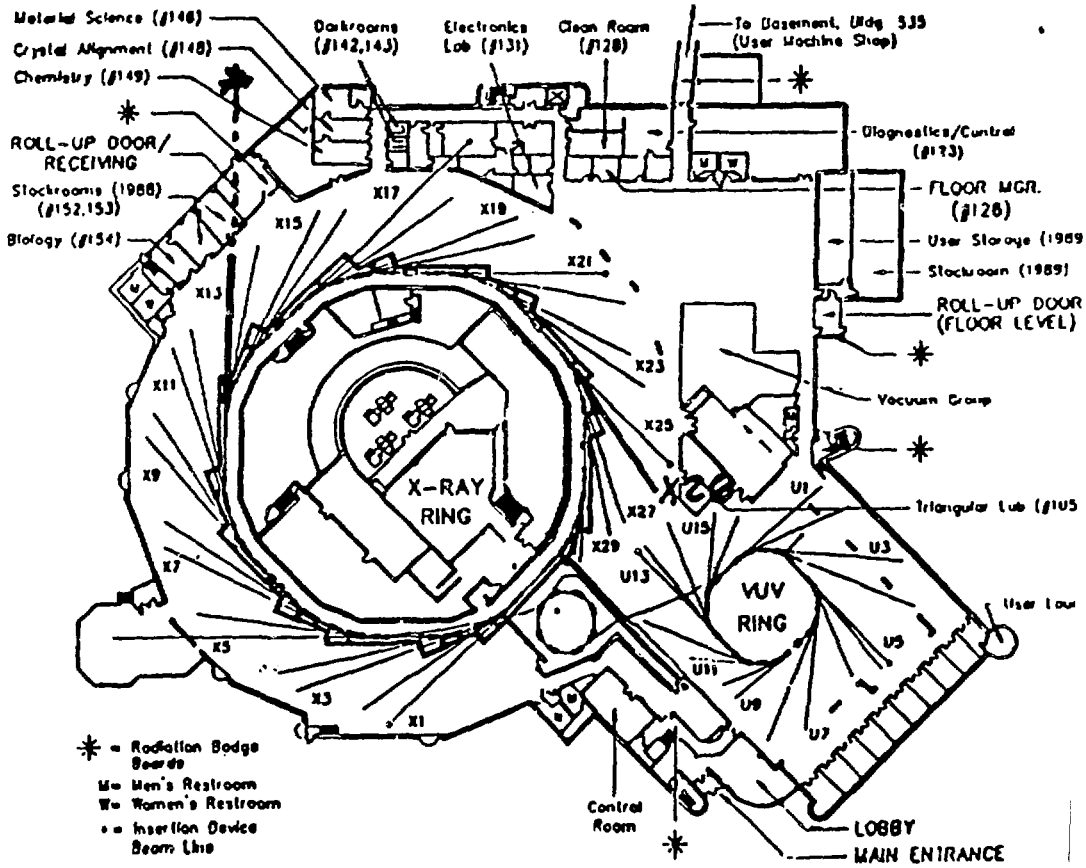


Fig. 3 is a schematic representation of the storage rings and beam lines of the NSLS x-ray and VUV beam lines. The location of beam port X26 is indicated.

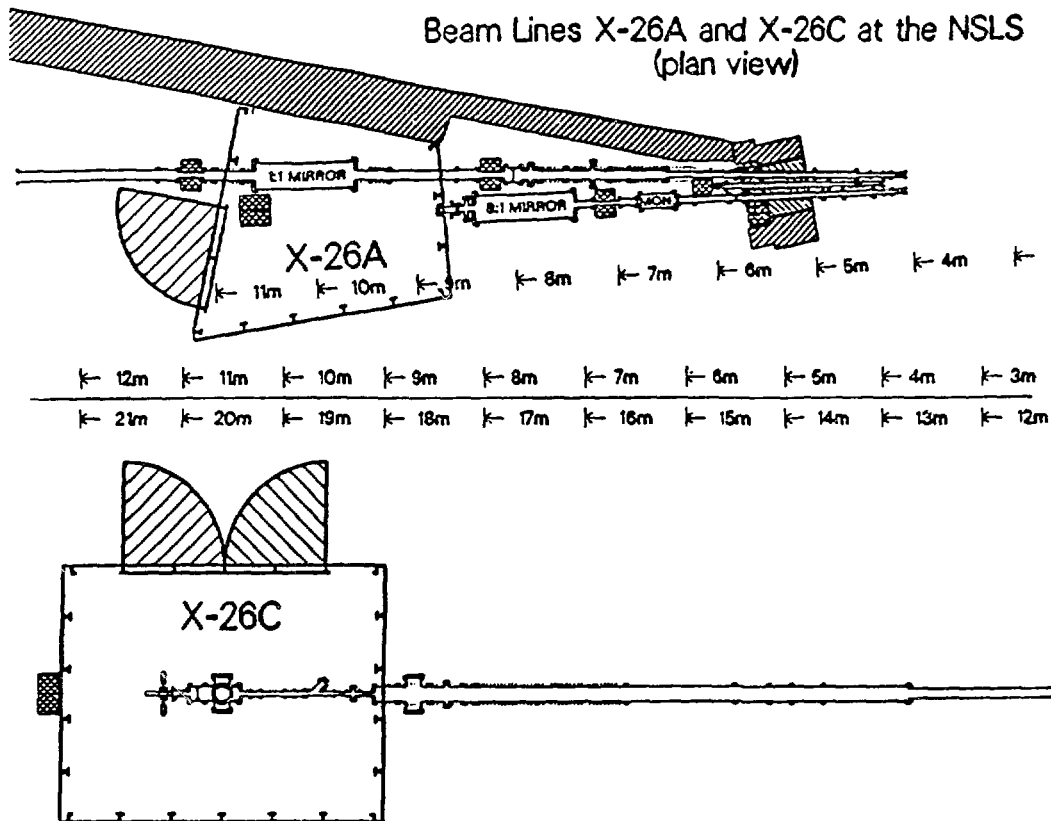
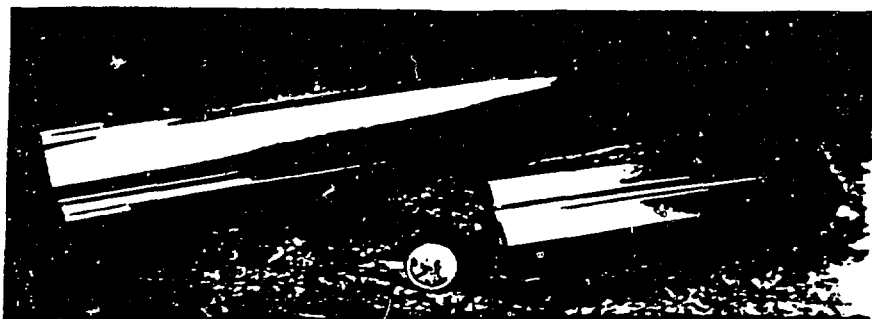


Fig. 4 gives the layouts of beam lines X26C and X26A on the X26 beam port of the NSLS x-ray ring at the NSLS. Note that neither beamline presently has a monochromator, but that each has an x-ray focussing mirror. On X26C a 1:1 cylindrical mirror is located at about 10 m from the photon source point to produce an image in the experimental hutch at about 20 m. On X26A an 8:1 ellipsoidal mirror is positioned at 8 m to produce a focal spot at about 9 m.

X-RAY FOCUSING MIRRORS

1:1 CYLINDRICAL.



8:1 ELLIPSOIDAL

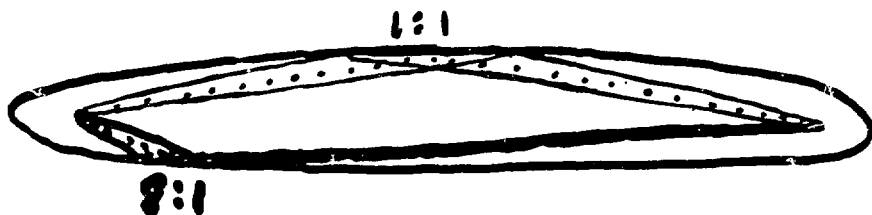


Fig. 5 shows the two focussing mirrors. The 1:1 mirror is made of Zerodur; is coated with platinum; is 60 cm long; and accepts 4 mr of horizontal radiation. The 8:1 mirror is made of electroless nickel; is coated with platinum; is 20 cm long; and accepts 2 mr of horizontal radiation. Both mirrors are used at an angle of incidence of about 4 mr giving a high-energy cutoff at about 15 keV. For a bending magnet or wiggler at the APS it might be desirable to try to focus the harder radiation above 15 keV. The cutoff can be moved to about 40 keV by lowering the angle of incidence to 2 mr. The APS experiments will more typically be located at 40 m from the ring with a mirror at 20 m. The hand-drawn sketch indicates schematically (in a two dimensional representation) how the mirrors operate. Imagine the ellipse rotated a few degrees each way about its long axis to produce sections of cylindrical and ellipsoidal surfaces. Reducing the incidence angle and increasing the distance between the foci amounts to stretching the whole ellipsoid and shrinking its minor radius. A 1:1 mirror of about the same length at 20 m from the ring with a 2 mr angle of incidence would accept only about 1 mr of horizontal radiation, instead of the 4 mr accepted on X26C.

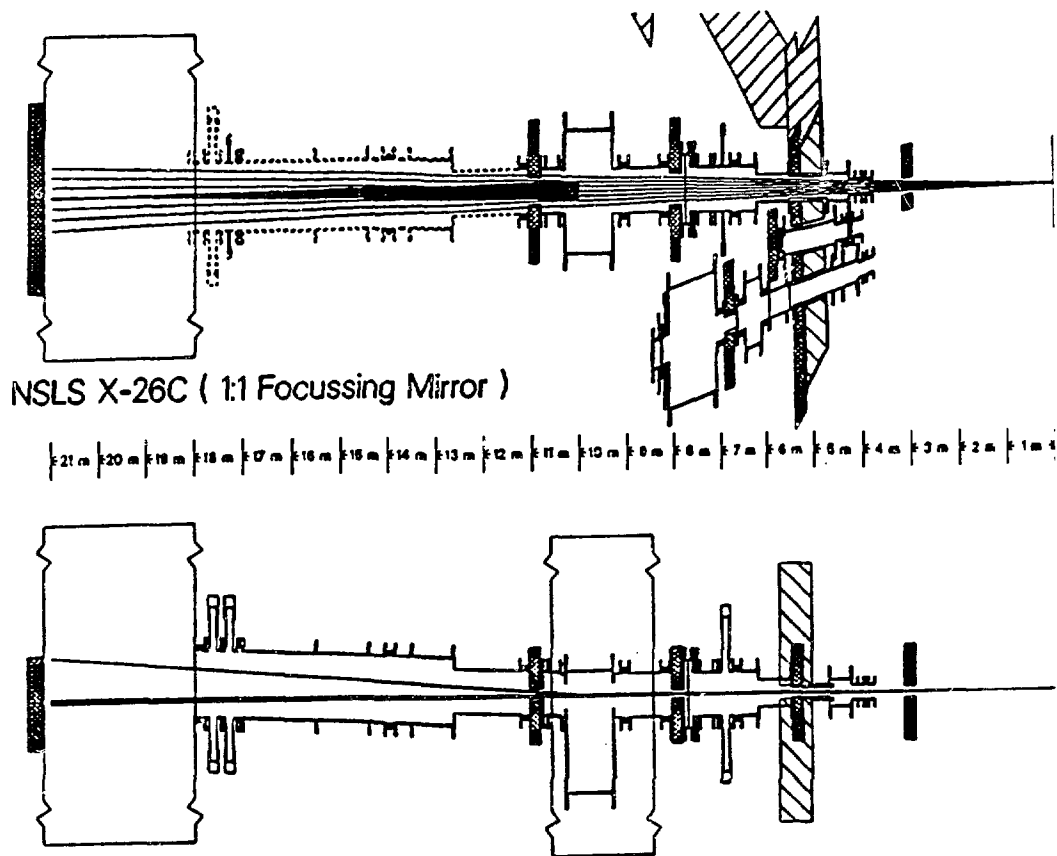


Fig. 6 shows an anamorphic drawing (transverse dimension greatly expanded) of the X26C beam line. The horizontal focussing action of the 1:1 mirror is indicated in the plan view (upper) and the vertical deflection is illustrated in the elevation view (lower).

Figs. 7-9 illustrate the measured performance of the 1:1 cylindrical x-ray mirror on X26C. Si(Li) x-ray detector was positioned at a forward scattering angle of 45° to measure photons scattered through air after passage through a $20 \times 20 \mu\text{m}$ pinhole.

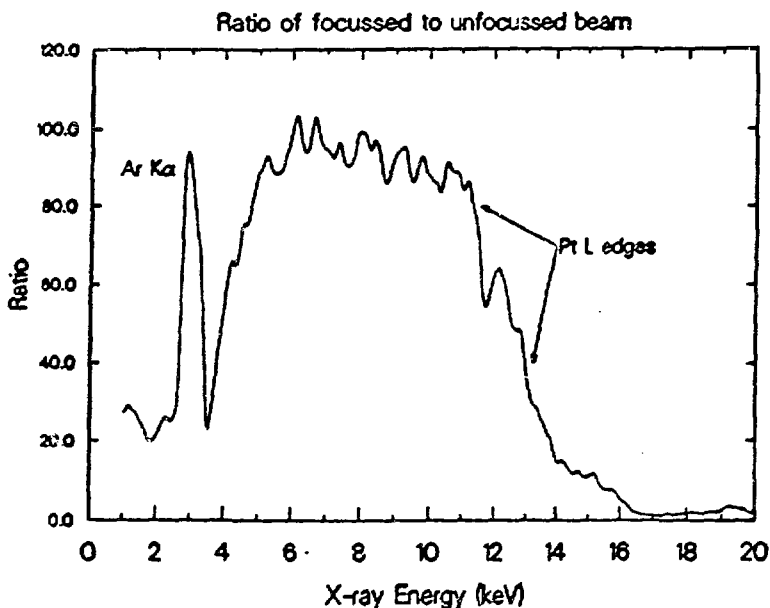
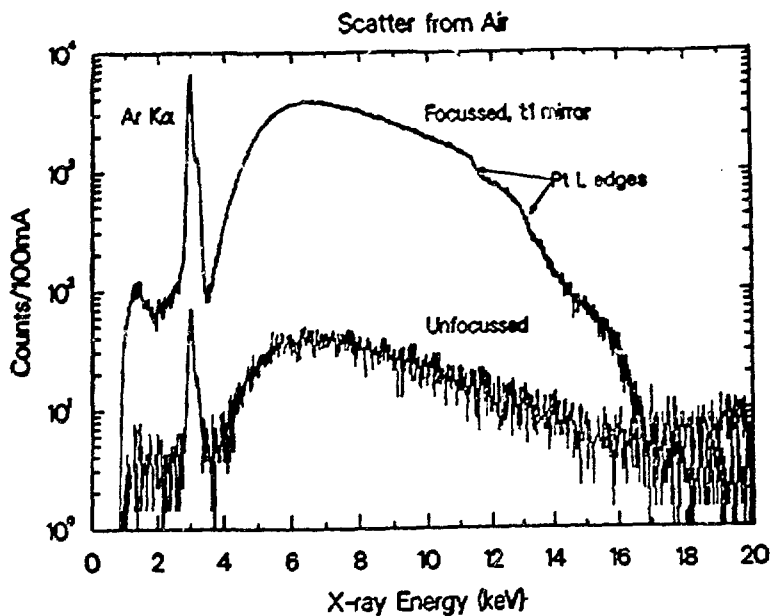


Fig. 7 (upper) shows the measured x-ray energy spectra for both unfocussed and focussed radiation with the pinhole positioned for maximum intensity. Fig. 7 (lower) displays the ratio of these two spectra. Note that an enhancement of two-orders of magnitude is realized over a wide range of photon energies and for the characteristic Ar K x-ray production produced from argon in the air. The dip at about 5 keV is artificial. Due to the low x-ray scattering cross sections near this photon energy there are very few counts in the scattered-radiation spectra.

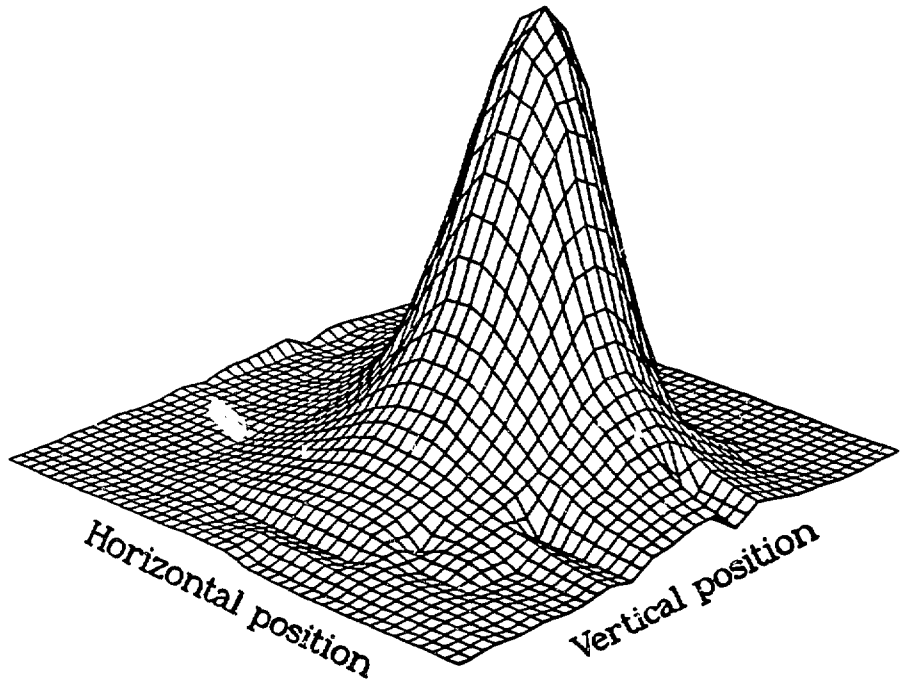


Fig. 8 is a two-dimensional line plot of the photon flux distribution produced at the focal point with the 1:1 mirror. Note that the focal spot is nearly round. The unfocussed horizontal image would have been about 8 cm wide. The full-width-at-half-maximum or 2σ of the focussed image was about 0.7 mm. Although the mirror specification called for no vertical focussing the vertical beam profile had a 2σ of 0.6 mm, while the unfocussed, was 1.8 mm. This factor of three reduction in vertical height is believed to result from slight concave curvature down the long axis of the mirror.

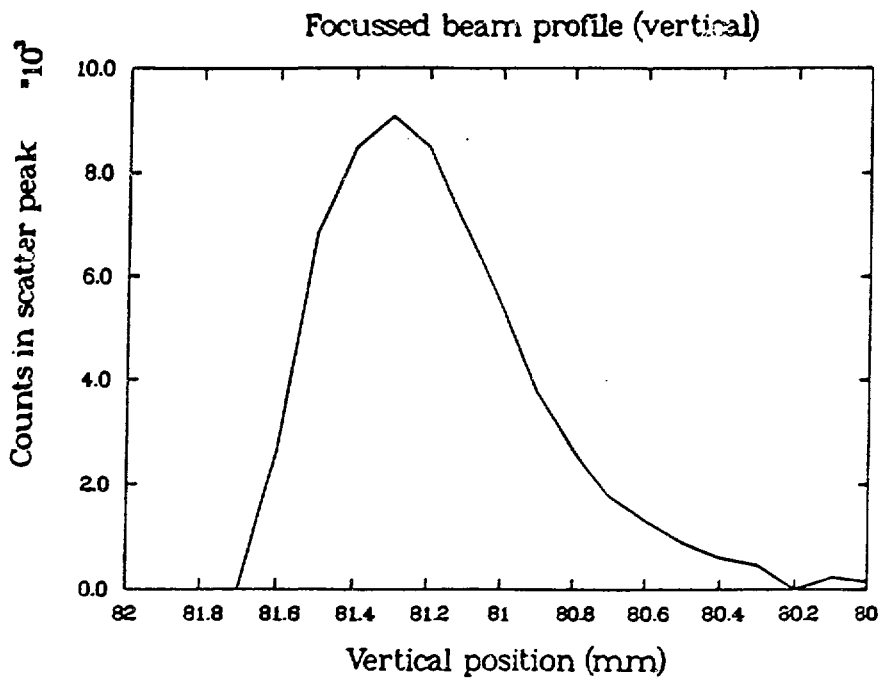
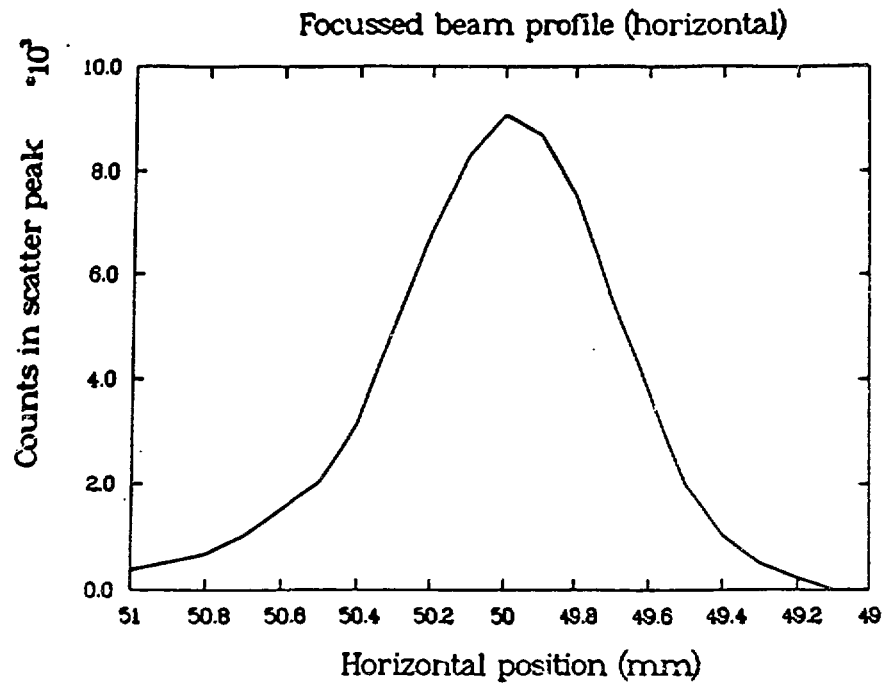


Fig. 9 shows the horizontal and vertical beam profiles at maximum intensity. The vertical profile is asymmetric only because it was clipped on one side by an aperture in the beam line.

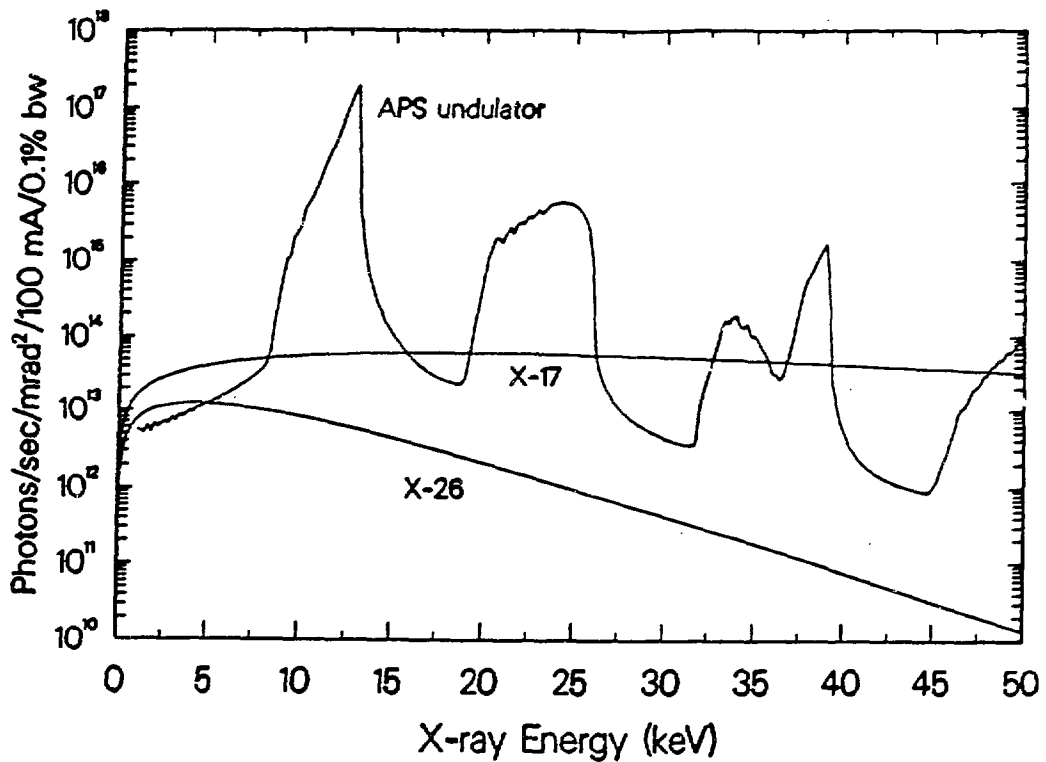


Fig. 10 shows the calculated photon-energy spectra for the undulator A of the APS compared to those for a typical bending magnet beam line (X26) and a super-conducting wiggler at maximum field strength of 5 Tesla (X17). The X17 spectrum (at 4.9 Tesla) is also typical of a generic bending magnet at the APS, although flux at the APS may be somewhat higher due to the lower source emittance. At a field strength of 1.1 Tesla, X17 produces essentially the same spectrum as an NSLS bending magnet port (e.g. x26). Clearly, an undulator provides much higher photon flux at soft x-ray energies than bending magnets or even super-conducting wigglers at the NSLS.

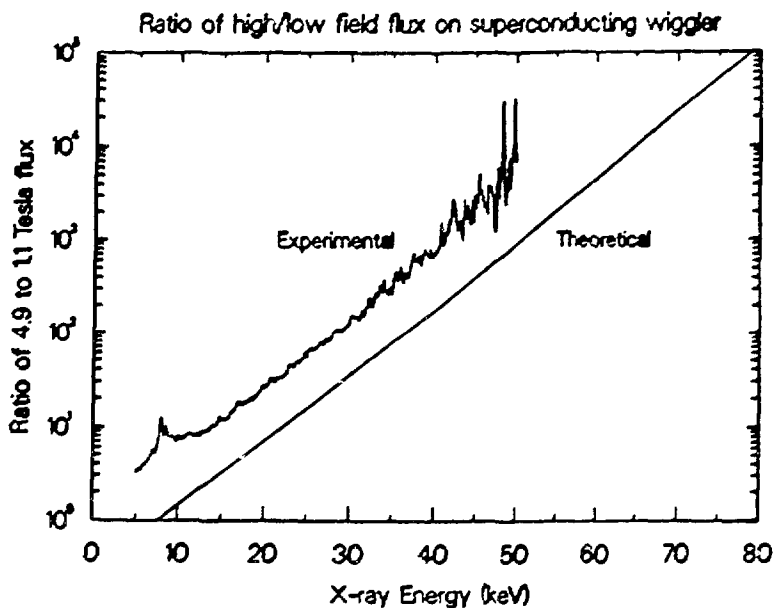
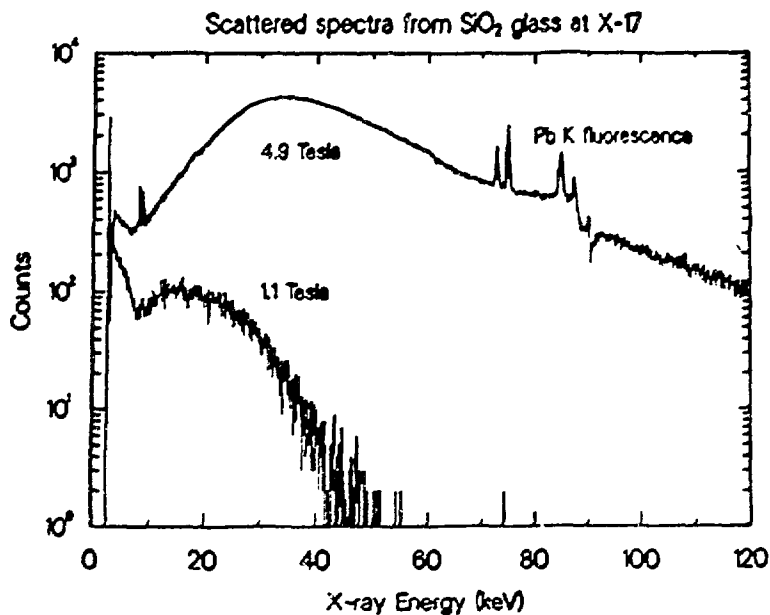


Fig. 11 is similar to Fig. 7, but here a measurement is made of unfocused x-ray scattering from a glass target on X17 at 1.1 and 4.9 Tesla with only 2 ma of stored electron beam. The upper spectrum shows the two radiation patterns and the lower compares the measured and predicted ratios. The energy dependence of the ratios agree well. The discrepancy in magnitude is attributed to either the loss of some beam when the magnet was ramped down from 4.9 to 1.1 Tesla or a normalization problem with the beam monitors at such low stored beam currents. Note that this direct comparison of the two radiation patterns under otherwise similar conditions indicates that an AF bending magnet beam line is clearly superior to a comparable NSLS line only at high x-ray energies above a few keV.

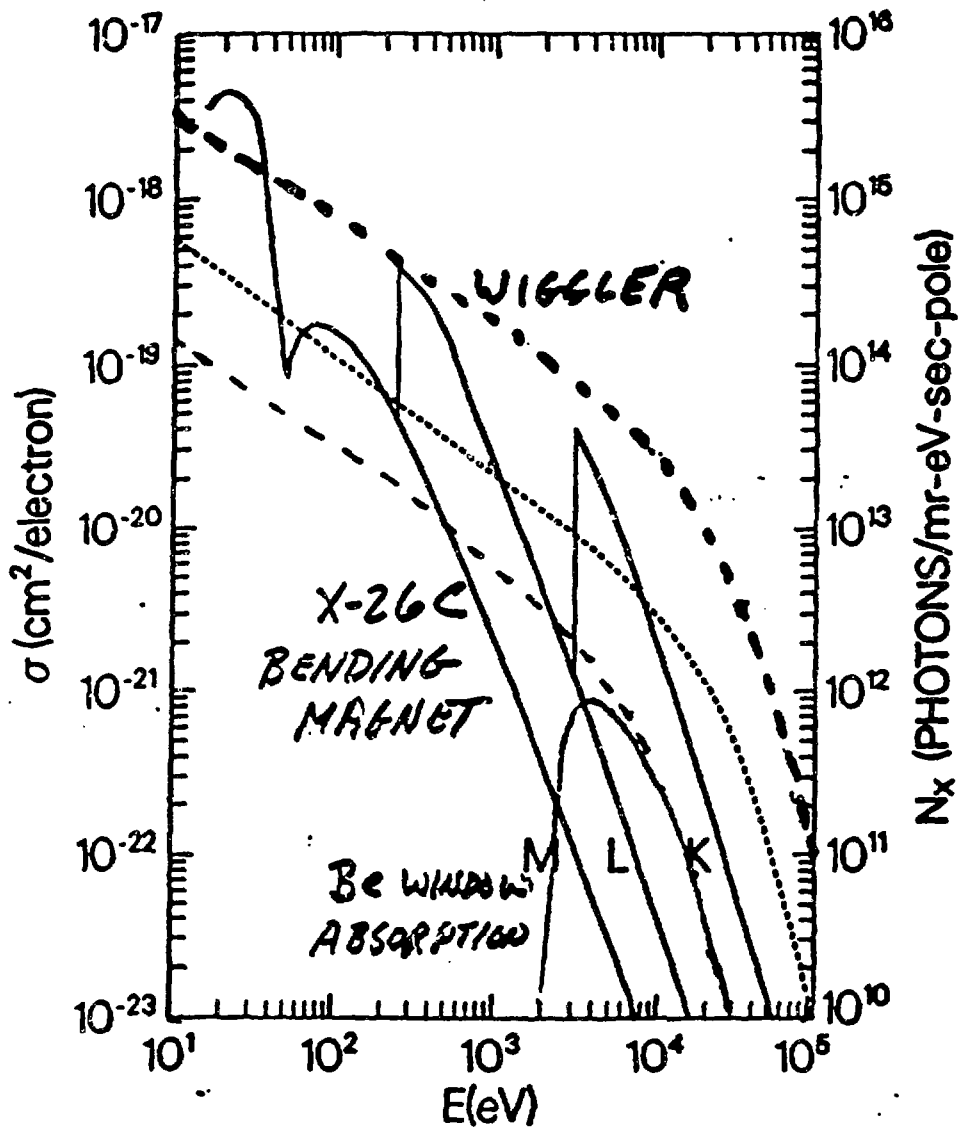
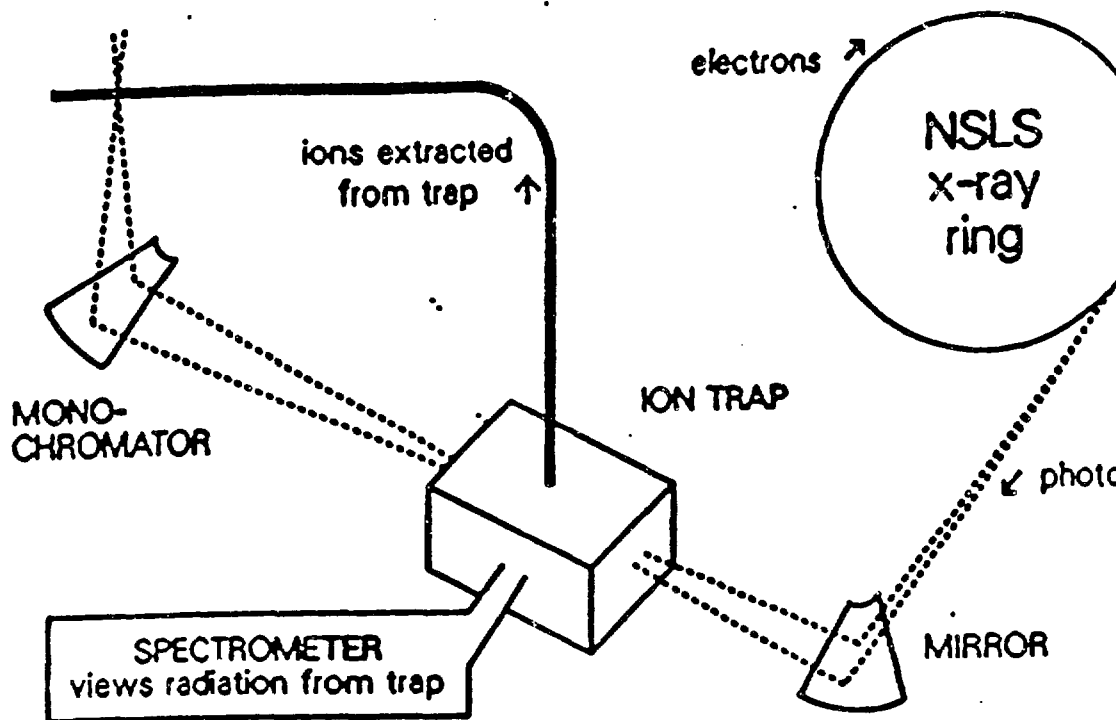


Fig. 12 shows the photon flux distributions for a typical NSLS bending magnet (X26C) and wiggler (X25), and the filtering effect of a Be window which absorbs low-energy photons. Note that the flux is plotted for photons in a 1 eV energy bandwidth rather than the more customary 0.1% wavelength bandwidth. Also indicated are the photoabsorption cross sections for the M-, L-, and K-shells of argon. Note that broadband radiation from either the bending magnet or wiggler span the entire range of binding energies for all electrons in argon. The same would be true at the APS for even the heaviest atoms.

PHOBIS: PHOTon Beam Ion Source



K. W. JONES, B. M. JOHNSON, M. MERON
PHYS. LETT. 97A, 377 (1983)

Fig. 13 illustrates the PHOBIS concept, which was proposed many years ago. The basic idea is to use an ion trap to hold ions in the path of broad-band synchrotron radiation to successively photoionize ions to higher and higher charge states. The first experimental demonstration of successive inner-shell photoionization in a Penning ion trap was recently achieved in a collaborative effort on NSLS beam line X26C. See the contribution to these proceedings by David A. Church.

NAPF

National Atomic Physics Facility

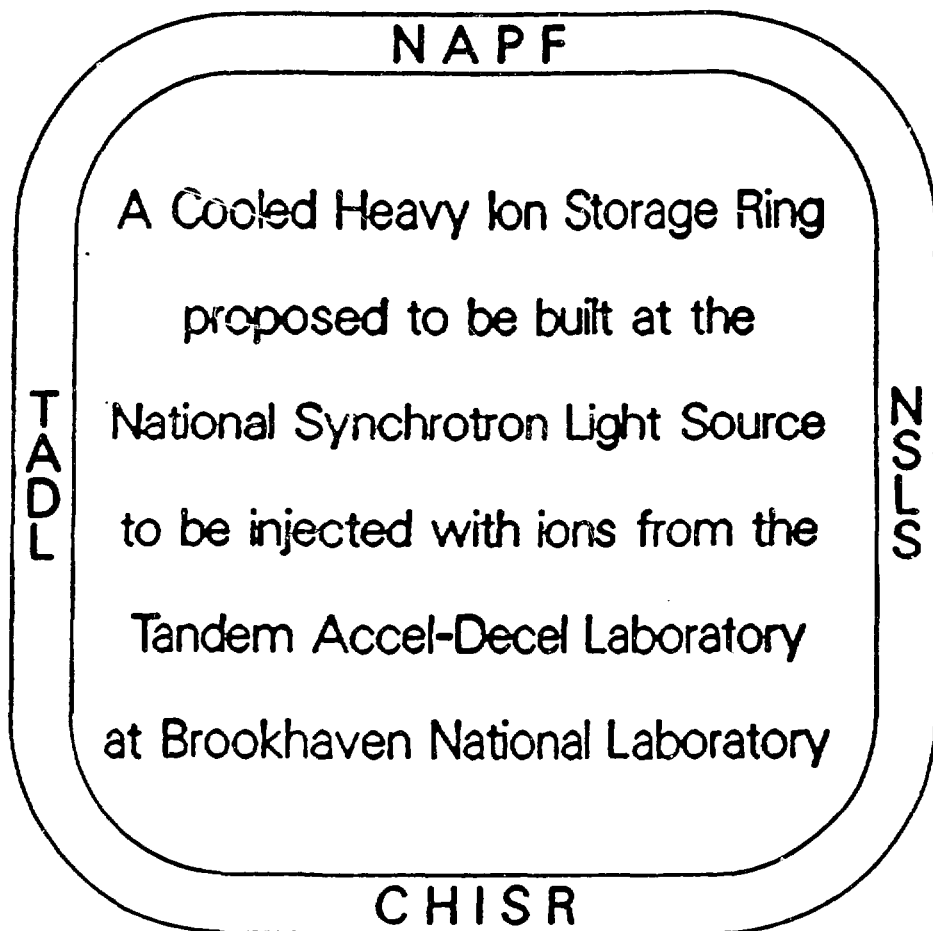


Fig. 14 introduces the basic elements of NAPF, the proposed National Atomic Physics Facility. Such a facility would be ideal for studies of the inner-shell photoionization of ions with hard x-rays, as well as a host of other ion-photon, ion-electron, and ion-atom investigations.

ATOMIC PHYSICS FOR THE 90's AND BEYOND

FUNDAMENTAL INTERACTIONS

- . THREE-BODY CONTINUUM COULOMB PROBLEM
- . QED EFFECTS AT HIGH-Z
- . STRONGLY PERTURBING INTERACTIONS
- . MANY-BODY INTERACTIONS/CORRELATION
- . ATOMS IN VERY HIGH FIELDS
- . TIME REVERSAL & PARITY NON-CONSERVATION IN ATOMS
- . FUNDAMENTAL CONSTANTS

POORLY UNDERSTOOD PROCESSES

- . COLLISIONS OF IONIZED SYSTEMS
- . CHARGE TRANSFER
- . ELECTRON COLLISIONS WITH HIGHLY-CHARGED IONS
- . PHOTON INTERACTIONS WITH IONS
- . ELECTRON-ION RECOMBINATION
- . LASER-ASSISTED PROCESSES: LASER + SYNCHROTRON, ETC.
- . DECAY OF MULTIPLY-EXCITED IONS
- . MANIFESTATIONS OF QUANTUM CHAOS

IMPORTANT APPLICATIONS

- . FUSION PLASMAS
- . ASTROPHYSICAL PHENOMENA
- . DEFENSE
- . EARTH AND PLANETARY ATMOSPHERES

2/8/89

Fig. 15 summarizes the scientific justification for NAPP. See also the the documents listed in the bibliography and the contribution to these proceedings by Steve Manson.

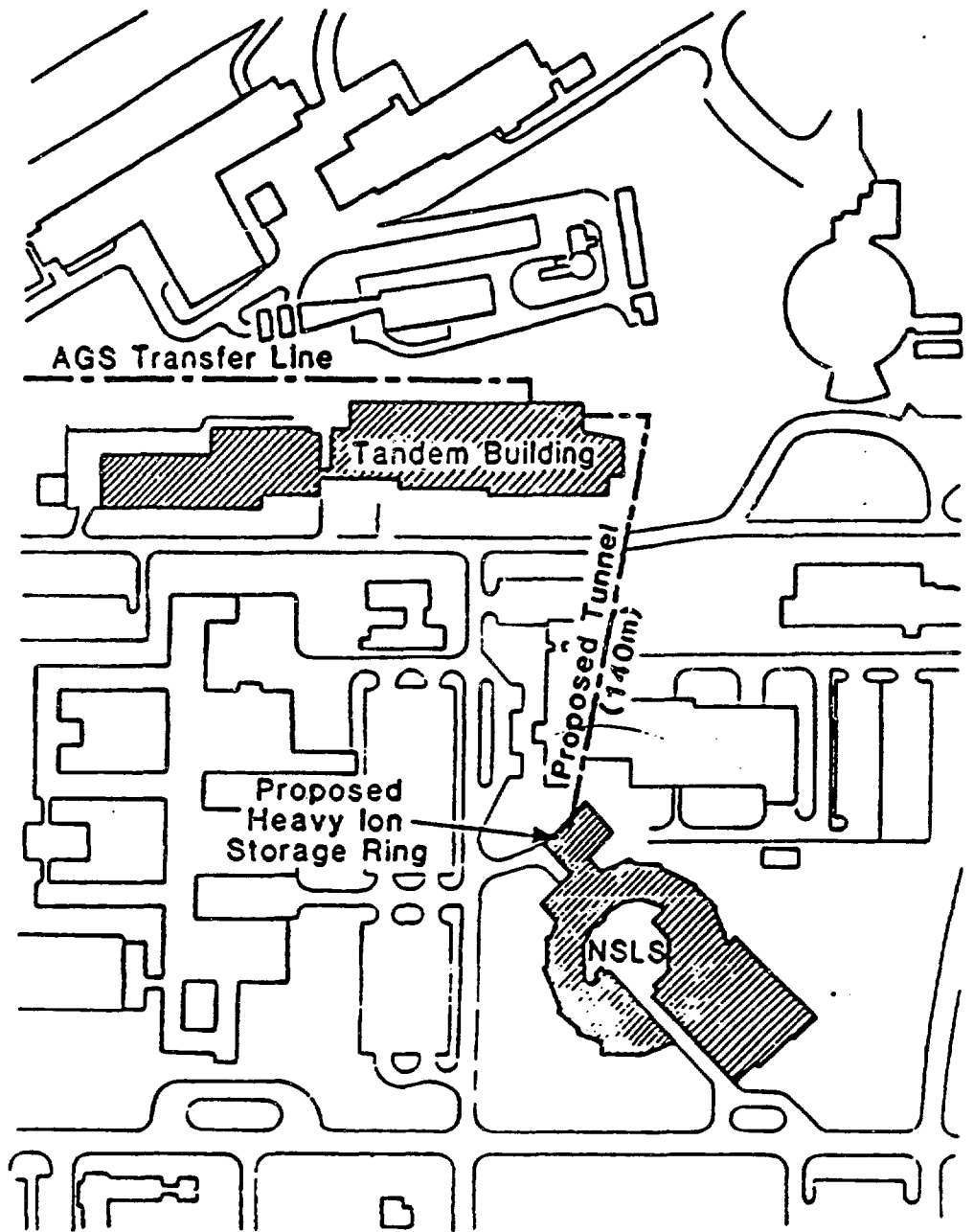


Fig. 16 indicates the proposed location of a heavy-ion transfer line from the BNL tandem facility to the NSLS. The existing transfer line to the BNL Alternating Gradient Synchrotron AGS is also shown.

CHISR: COOLED HEAVY ION STORAGE RING

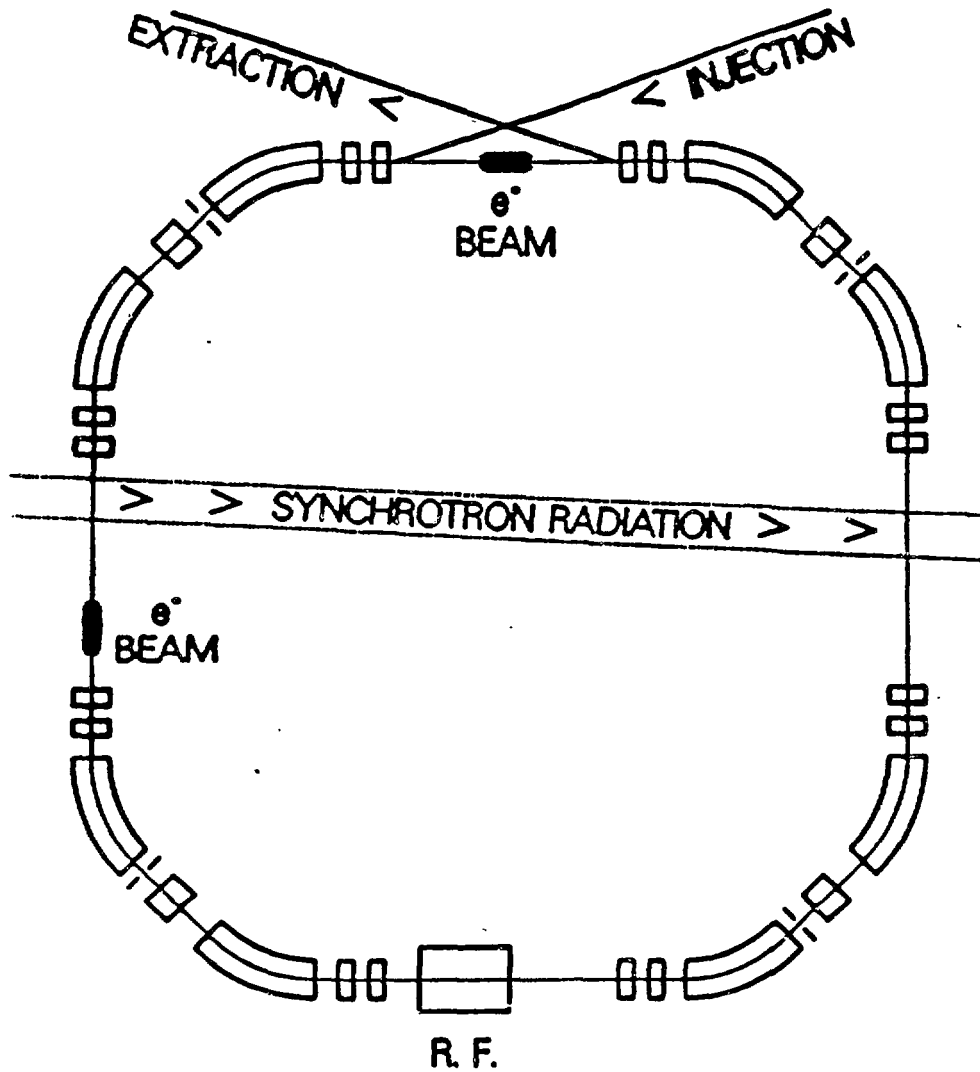


Fig. 17 gives a schematic diagram of the photon beam from the NSLS x-ray ring interacting with stored heavy ions.

Beam Line X-13 at the NSLS

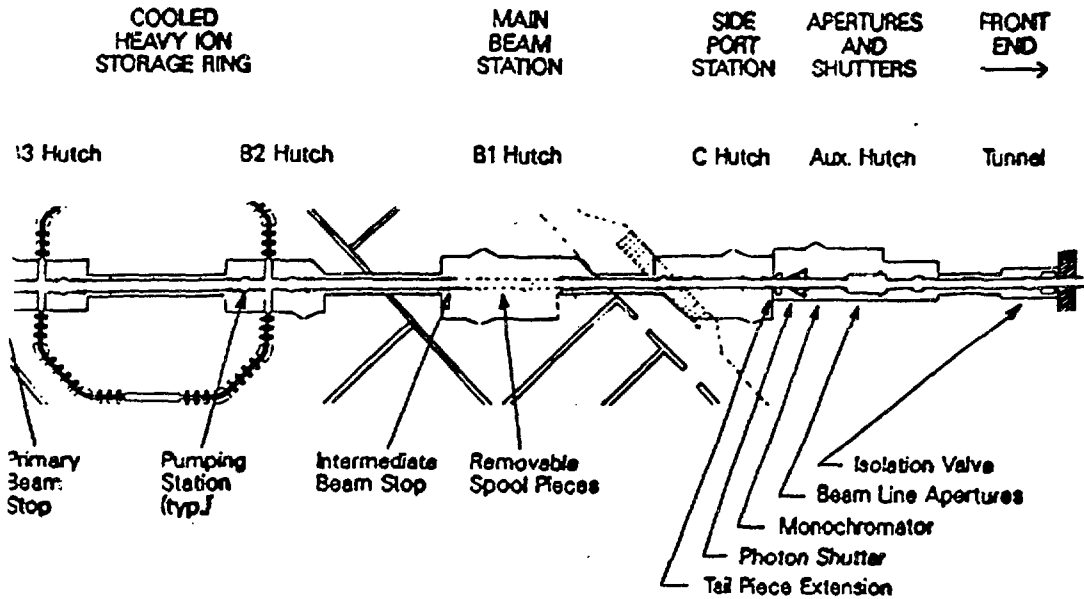


Fig. 18 shows some details of the design of a specific superconducting-wiggler beam line proposed for port X13 at the NSLS. Note the provision for independent experiments on the photon beam line during time periods when the heavy-ion storage ring would not be available for SR experiments.

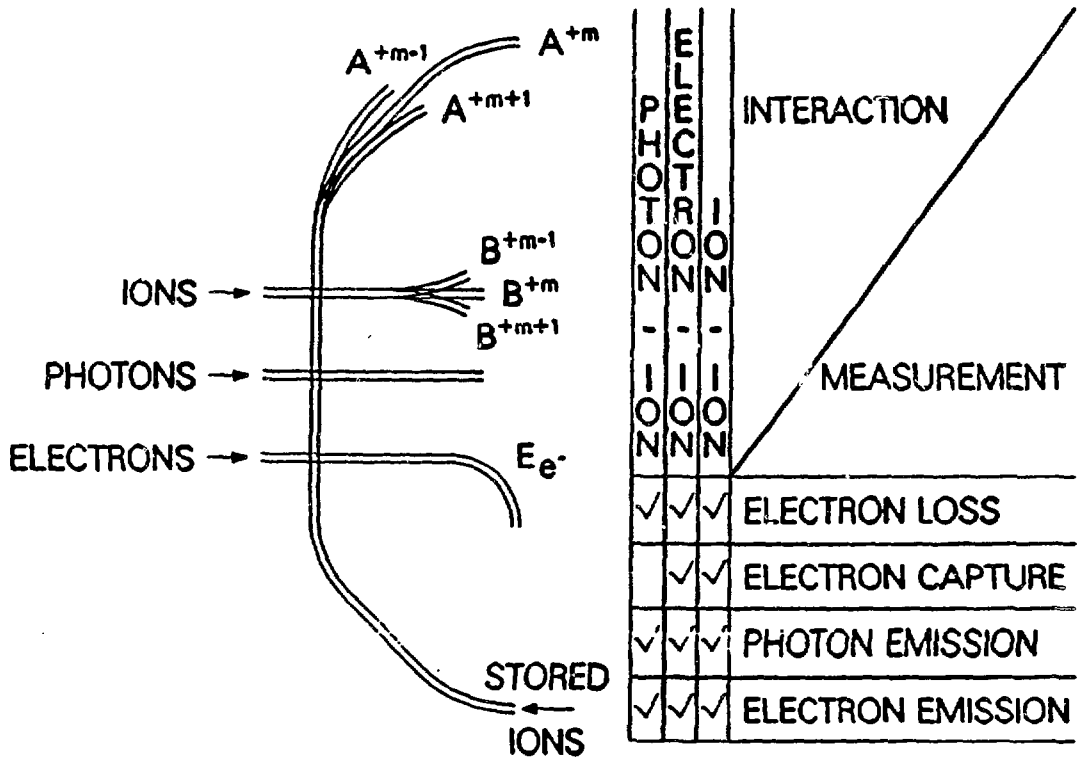
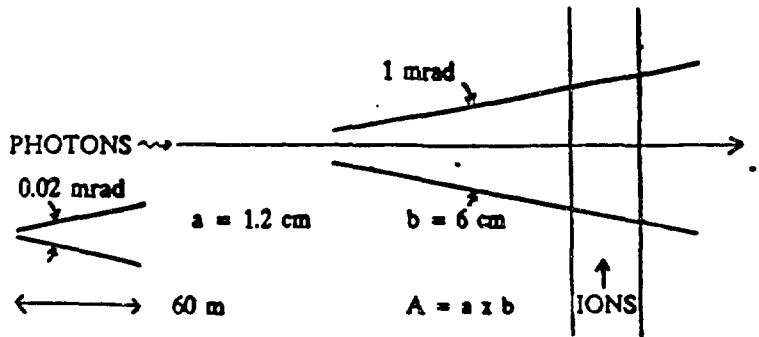


Fig. 19 illustrates the wide range of measurements that would be possible in studying ion-photon, ion-electron, and ion-ion interactions at NAPF.

PHOTON-ION LUMINOSITY

PHOTON BEAM INTERACTING WITH STORED HEAVY IONS:



$$L = \frac{N_{\text{HI}} N_{\text{P}}}{A} f_{\text{enc}}$$

$$N_{\text{P}} f_{\text{enc}} = 1 \times 10^{14} \text{ photons/sec-mrad}$$

BANDWIDTH OF 0.1 %

DEBUNCHED: $N_{\text{HI}} = N_{\text{TOT}} \frac{b}{2 \pi R}$

BUNCHED, $l > b$: $N_{\text{HI}} = N_{\text{TOT}} \frac{b}{M l}$

BUNCHED, $l < b$: $N_{\text{HI}} = \text{NUMBER OF IONS IN ONE BUNCH}$

Fig. 20 describes the figure of merit for a crossed photon - heavy ion beam experiment - namely, the photon - ion luminosity. The parameter f_{enc} is the frequency of encounter, which is typically 1 M Hz or 10^6 passes per second of the stored heavy ions.

Consider K-shell Photoionization of Cu ¹¹⁺

Assume photon energy resolution $\Delta E/E$ of 0.1%
(better than 8 eV) and photon flux of 10^{14} Hz.

SIGNAL: (K-shell photoionization events)

Cross Section
(near K-edge) $3.0 \times 10^{-20} \text{ cm}^2$

Luminosity
(Ion-photon interactions) $4.3 \times 10^{20} \text{ cm}^{-2} \text{ s}^{-1}$

SIGNAL Rate 13 Hz

BACKGROUND: (Interactions with ambient gas, 10^{-11} Torr)

Cross Section
(K-shell vacancy production) $2 \times 10^{-22} \text{ cm}^2$

Luminosity
(2.9 MeV/u beam energy) $2 \times 10^{26} \text{ cm}^{-2} \text{ s}^{-1}$

BACKGROUND Rate 4000 Hz

SIGNAL/BACKGROUND ratio $13/4000 = 0.3\%$

Fig. 21 begins a calculation of expected signal to noise ratios for a specific photoionization measurement in CHISR at NAPS (to be continued in the next figure).

K-shell Photoionization of Cu ¹¹⁺ (Continued)

Synchrotron Radiation is PULSED.

NSLS x-ray ring normally operated with 25 bunches.

Bunch Width (4σ)	0.6 - 1 ns
Revolution Frequency	567.7 ns
Duty Factor	0.026 - 0.044
Typical Duty Factor	0.03

SIGNAL/BACKGROUND ratio $13/(4000 \times 0.03) = 11\%$

Similar calculations for outer-shell ionization of Cu ions yield SIGNAL/BACKGROUND ratios of 3 to 9%.

CONCLUSION

CHISR experiments on the photoionization of ions (both inner- and outer-shell) are feasible.

Fig. 22 the continuation of the calculation begun in the preceding figure. Note that the conclusion would be even more valid for a similar proposal at the APS. Instead of a long and costly transfer line from ATLAS, an ECR ion source and linac near the CHISR could be used for injection.

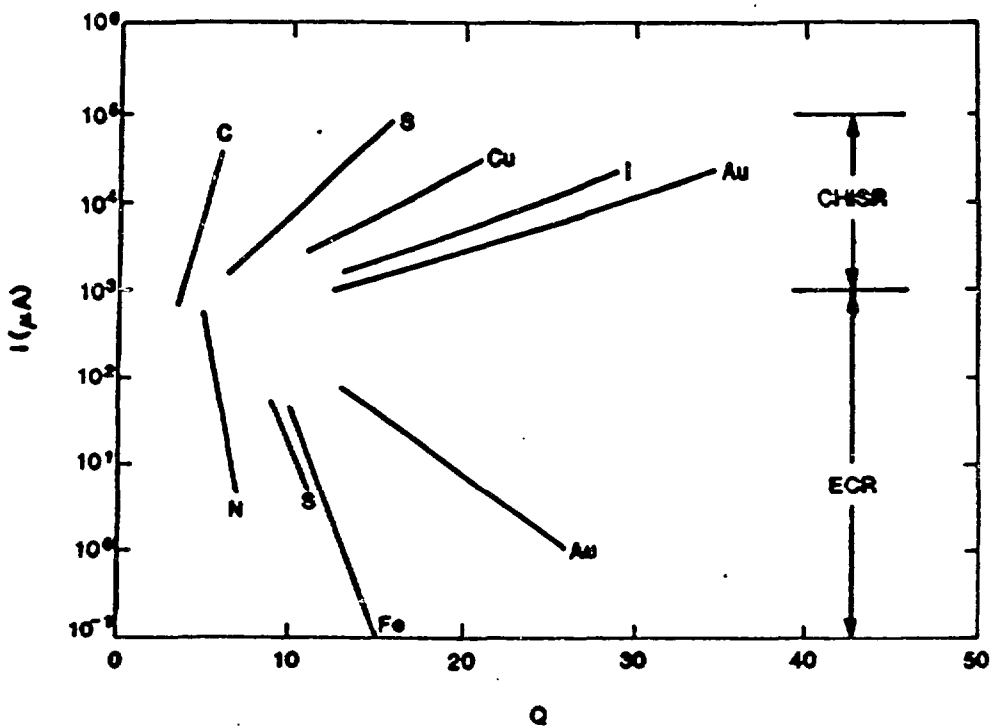


Fig. 23 compares effective beam currents for a Cooled Heavy-Ion Storage Ring versus an Electron-Cyclotron Resonance Ion Source. The overall magnitudes are very dependent on specific assumptions about the performance of each type of ion source, but the trend versus increasing charge state is generic. ECR sources are competitive at low charge states and for light to medium Z elements, but CHISR clearly wins as the charge state and mass of the ion is increased.

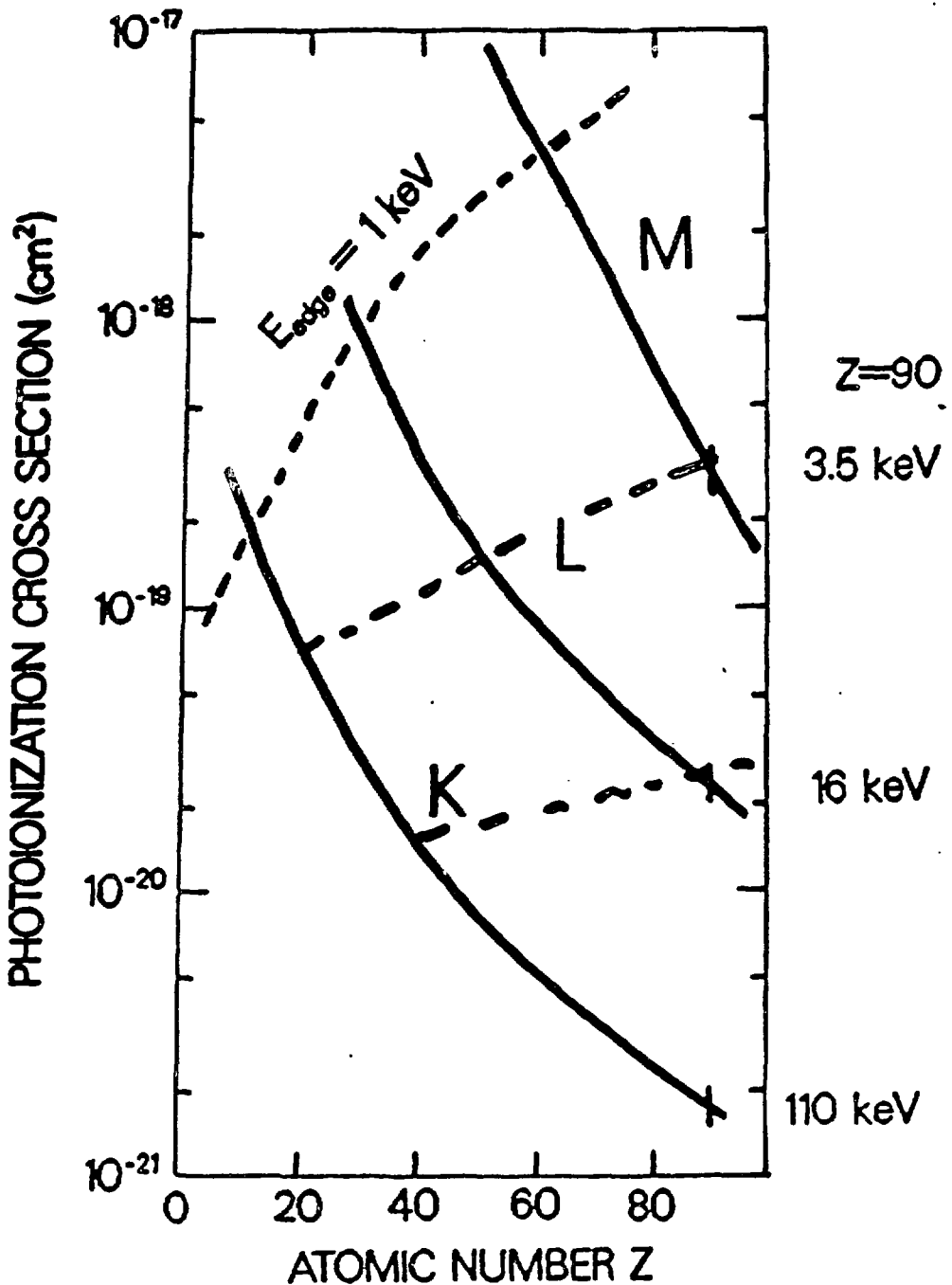


Fig. 24 gives plots of photoionization cross sections versus Z for K-, L-, and M-shells of all elements. Note that the elements and shells covered by different ranges of soft and hard x rays are indicated with dashed lines. While inner-shell studies over a wide range of low to medium Z ions can be performed with soft x rays, such experiments on heavier atoms require the much harder x rays available in abundance at the APS or on a superconducting wiggler at the NSLS.